

Electrotransfer parameters as a tool for controlled and targeted gene expression in skin

Spela Kos¹, Tanja Blagus¹, Maja Cemazar^{1,2}, Ursa Lamprecht Tratar¹, Monika Stimac¹, Lara Prosen¹, Tanja Dolinsek¹, Urska Kamensek¹, Simona Kranjc¹, Lars Steinstraesser³, Gaëlle Vandermeulen⁴, Véronique Prémat⁴ and Gregor Sersa¹

Skin is an attractive target for gene electrotransfer. It consists of different cell types that can be transfected, leading to various responses to gene electrotransfer. We demonstrate that these responses could be controlled by selecting the appropriate electrotransfer parameters. Specifically, the application of low or high electric pulses, applied by multi-electrode array, provided the possibility to control the depth of the transfection in the skin, the duration and the level of gene expression, as well as the local or systemic distribution of the transgene. The influence of electric pulse type was first studied using a plasmid encoding a reporter gene (DsRed). Then, plasmids encoding therapeutic genes (IL-12, shRNA against endoglin, shRNA against melanoma cell adhesion molecule) were used, and their effects on wound healing and cutaneous B16F10 melanoma tumors were investigated. The high-voltage pulses resulted in gene expression that was restricted to superficial skin layers and induced a local response. In contrast, the low-voltage electric pulses promoted transfection into the deeper skin layers, resulting in prolonged gene expression and higher transgene production, possibly with systemic distribution. Therefore, in the translation into the clinics, it will be of the utmost importance to adjust the electrotransfer parameters for different therapeutic approaches and specific mode of action of the therapeutic gene.

Molecular Therapy—Nucleic Acids (2016) 5, e356; doi:10.1038/mtna.2016.65; published online 30 August 2016

Subject Category: Gene Insertion, Deletion & Modification

Introduction

Gene electrotransfer (GET) is a safe and efficient nonviral gene delivery method based on electroporation, *i.e.*, the application of controlled electric pulses to cells or tissues.¹ The method has been used in gene therapy to deliver naked DNA or RNA to different tissues, including the skin.^{2–4} Specifically, skin is an attractive target for gene therapy and vaccination due to its easy accessibility, large treatment area and the presence of many antigen-presenting cells, which are critical for eliciting an effective immune response.⁵

Skin GET has been used to effectively elicit both local and systemic expression of transgenes and has been used in many medical applications, including vaccination,^{2,6–9} wound healing,^{10–12} and cancer treatment,^{3,13} as well as local and systemic skin disorders.¹⁴ Due to the increasing use of skin GET for medical purposes, the gene expression induced in the skin should be well characterized and controlled. An important aspect of regulating the duration and the effects of gene delivery is the targeted transfection of specific skin layers.

Skin is a complex tissue that is divided into different layers consisting of different cell types.^{14,15} The diversity of cell types in skin could be of the utmost importance in gene therapy and DNA vaccination because different cell types can theoretically elicit different responses to gene transfection. Genes transfected into muscle cells can have long-term expression

because muscle fibers rarely divide, while genes transfected into keratinocytes show short-term expression due to the faster cell turnover.^{14,16} In addition to the duration and level of gene expression, the specific targeting of different types of skin cells or layers could influence the local, paracrine or systemic effectiveness of the gene therapy. If keratinocytes in superficial skin layers are transfected, local or paracrine action of the transgene is expected. However, when cells in deeper skin layers are transfected, a systemic effect can also be expected due to shedding of the protein into the bloodstream. This presumption was confirmed in our previous study, where with noninvasive electrodes and varied electrotransfer parameters, local or systemic distribution of the therapeutic molecule doxorubicin was observed.¹⁷ In this study, we hypothesized that varied parameters of GET applied with the same electrodes could affect the localization and expression of the delivered transgene.

The transfection of a specific region in the skin depends on different parameters, such as electrode selection, electrical parameters,^{14,18–20} injection technique, animal species, dose of plasmid administered, and plasmid design.²¹ The aim of our study was to evaluate the different parameters of electrotransfer as a tool for targeted gene delivery to different layers of the skin and to distinct between the local or systemic effects of such gene therapy. As in our previous study for the delivery of small molecules into skin,¹⁷ pulses were applied using a multi-electrode array (MEA). Two different types of

¹Department of Experimental Oncology, Institute of Oncology Ljubljana, Ljubljana, Slovenia; ²University of Primorska, Faculty of Health Sciences, Izola, Slovenia; ³Department of Plastic Surgery, Burn Center, BG University Hospital Bergmannsheil, Ruhr University Bochum, Bochum, Germany; ⁴Université Catholique de Louvain, Louvain Drug Research Institute, Advanced Drug Delivery and Biomaterials, Brussels, Belgium. Correspondence: Maja Cemazar, Department of Experimental Oncology, Institute of Oncology Ljubljana, Zaloska 2, SI-1000 Ljubljana, Slovenia. E-mail: mcemazar@onko-i.si or Gregor Sersa, Department of Experimental Oncology, Institute of Oncology Ljubljana, Zaloska 2, SI-1000 Ljubljana, Slovenia. E-mail: gsersa@onko-i.si

Keywords: controlled delivery; electrical parameters; gene electrotransfer; multi-electrode array; plasmid DNA; skin

Received 24 May 2016; accepted 7 July 2016; published online 30 August 2016. doi:10.1038/mtna.2016.65

electric pulses were compared: (i) short, high-voltage (HV) pulses and (ii) long, low-voltage (LV) pulses. Mouse skin was selected as the model to evaluate the effects of varied GET parameters. Namely, mouse skin has an additional subcutaneous muscle layer called the *panniculus carnosus*. This layer enables us to distinguish between superficial and deeper transgene delivery as well as to study the therapeutic outcome of GET. We anticipated that with different electrotransfer parameters, we could control the depth of transfection into the skin and the level and the duration of gene expression, as well as whether the transcribed protein distribution was systemic or local. We found that the GET parameters could be adjusted for the desired transgene mode of action (*i.e.*, local or systemic) and optimized for maximum therapeutic effectiveness, when MEA is used. Similar effects could be anticipated in human skin, where the transfection of deep, well-vascularized skin layers could lead to systemic transcribed protein distribution.

Results

Electrical pulses influenced both the intensity and the duration of gene expression

The intensity and duration of DsRed reporter gene expression after intradermal plasmid injection and the application of LV and HV electric pulses to the skin were monitored using noninvasive fluorescence imaging of the transfected mouse skin. When the plasmid was injected without the electroporation as a delivery method, the fluorescence signal was not detected. When HV electric pulses were applied, the expression peaked at day 2 post-treatment and then declined for the next 2 weeks. The onset of gene expression was similar with LV electric pulses, but after 2 days, the fluorescence signal started to blur and spread in the shape of muscle cells, indicating the transfection of deeper skin layers (Figure 1a). Fluorescence was detected for up to 5 days longer with LV pulses than with HV pulses (Figure 1b).

The transfection of deeper skin layers with LV pulses was further supported by the observation that no expression was observed after the subcutaneous injection of plasmid DNA followed by HV pulses. In contrast, significant fluorescence signals were detected after the administration of LV pulses (Figure 1c). To further validate these results, histological analysis of the excised skin was performed.

The depth of transfection of pCMV-DsRed was evaluated by imaging the fluorescence of frozen skin sections. The first samples were excised at day 2 post-treatment. After intradermal injection of pCMV-DsRed followed by HV pulses, DsRed expression was observed in upper layers of the skin (*i.e.*, epidermis and dermis), while LV pulses promoted transfection in the epidermis, dermis and subcutis, including the deepest muscle layer (*panniculus carnosus*). In the skin sections excised at day 6 after the HV pulse treatment, pCMV-DsRed gene expression was not detected. On the contrary, the fluorescence signal was still observed in the upper layers, as well as in the muscles, after the application of LV pulses (Figure 2). Therefore, the histological analysis proved the effect of different electrical parameters on the duration of transgene production and the selective transfection of different skin layers, which was observed by noninvasive fluorescence imaging of the transfected skin.

Local and systemic expression of the IL-12 therapeutic gene was influenced by the applied pulses

The gene expression of IL-12 in the skin was evaluated by qRT-PCR analysis after the intradermal injection of pORF-mIL-12, which was followed by the application of LV and HV pulses. Under both electrical conditions, *i.e.*, LV and HV pulses, GET resulted in significantly increased expression levels of IL-12 mRNA at day 2 post-treatment, compared with the untreated control group (Figure 3a). Four days after GET, the IL-12 mRNA levels rapidly decreased. These results illustrate notable gene expression in the skin with brief mRNA persistence.

Subsequently, the protein levels were measured after intradermal GET of the therapeutic plasmid coding for IL-12. The local protein expression was measured in excised skin samples, while the systemic distribution of IL-12 was determined in mouse serum. Locally in the skin (Figure 3b), the application of LV pulses resulted in significantly higher IL-12 production compared with the application of HV pulses. In both cases, the expression peaked at day 2 after the treatment ($1,213.3 \pm 71.8$ pg/ml for LV; 553.5 ± 99.0 pg/ml for HV), and it steadily decreased for the next few days. At the last detection time point, 6 days post-treatment, IL-12 was still detectable in low concentrations. In serum samples (Figure 3c), high concentrations of IL-12 were measured 2 days after the delivery of LV pulses (379.0 ± 80.3 pg/ml). The systemic distribution rapidly decreased over the next 2 days. In contrast, after the delivery of HV pulses, the systemic concentration of IL-12 was minimal, significantly lower compared with the application of LV pulses and completely reduced at day 6 post-treatment. Therefore, these results suggest that transgene is produced locally in the skin after intradermal injection of pORF-mIL-12 followed by the application of LV or HV pulses, while only LV pulses promote systemic protein distribution, whereas HV pulses restrict the expression locally in the skin.

The antitumor effect is stronger after IL-12 GET using LV pulses

The antitumor effectiveness of GET with plasmid DNA encoding IL-12 was evaluated on the B16F10 melanoma tumors as proof of principle. IL-12 is responsible for the antiangiogenic effect of the therapy as well as for local and systemic immunomodulation.^{13,22} The antitumor efficiency of systemically distributed IL-12 was presented in previous studies with GET into the mouse muscle.^{23,24} This time, tumor growth was monitored after the peritumoral injection of plasmid DNA followed by the application of LV or HV pulses. A significant increase ($P < 0.05$) in mouse survival was observed in both HV and LV pulse groups compared with that in the untreated control group and the group treated with the control plasmid pControl. The LV pulses prolonged mouse survival up to 8 weeks post-treatment. The HV pulses prolonged survival up to 3 weeks after the therapy (Figure 4). Therefore, the LV pulses, which induce the transfection of the deeper *panniculus carnosus* layer and also lead to the systemic distribution of IL-12, exhibited significantly ($P < 0.05$) better antitumor effectiveness compared with the HV pulses, which only exerted local effectiveness.

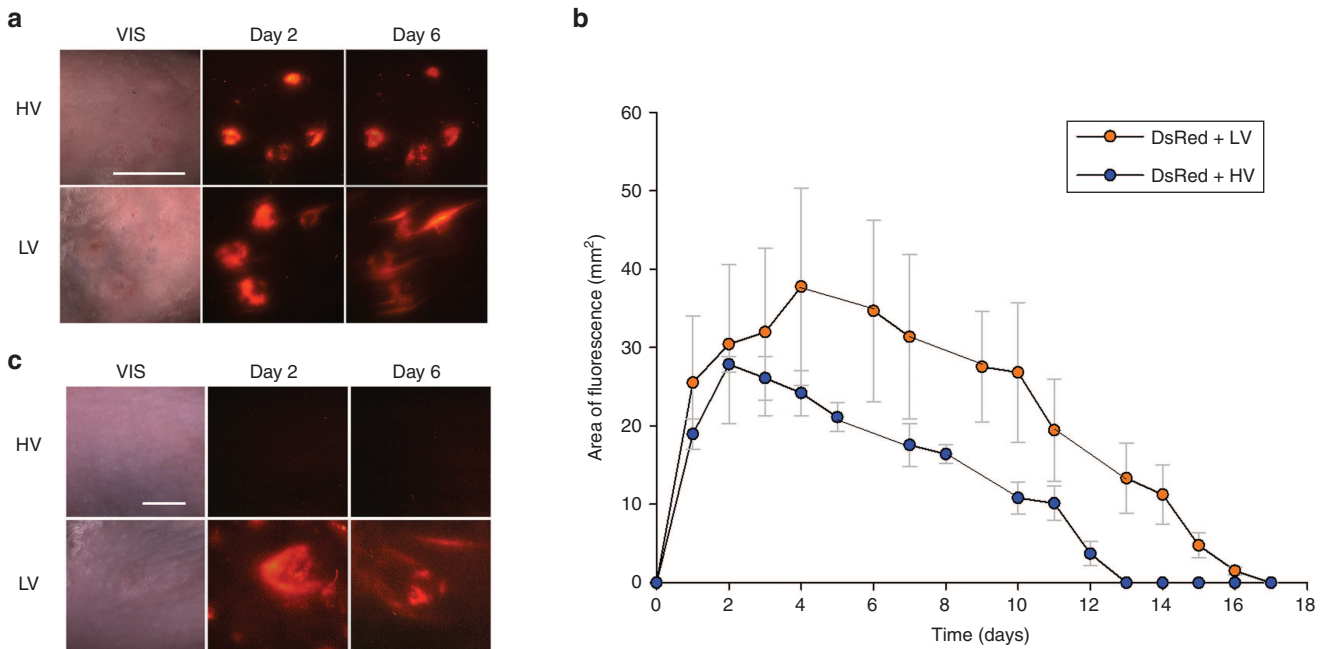


Figure 1 Fluorescence of DsRed protein following electrotransfer of the reporter plasmid coding for DsRed in mouse skin. (a) Representative images of the treated region of mouse skin showing the increased fluorescence signal due to *intra*dermal injection of plasmid DNA followed by the application of high-voltage (HV) or low-voltage (LV) pulses. Images were acquired using the fluorescence stereomicroscope at the designated times. Scale bar: 5 mm. (b) Fluorescence intensity of DsRed protein obtained in mouse skin at different time points. Fluorescence was measured after multiple *intra*dermal injections of pCMV-DsRed, followed by the application of HV or LV pulses. To measure the fluorescence intensity, images were analyzed using the same exposure criteria; $n = 6$ mice per group. Error bars indicate standard error of the mean. (c) Representative images of a treated mouse skin region showing increased fluorescence signal due to *subcutaneous* injection of plasmid DNA followed by the application of HV or LV pulses. Images were captured using the fluorescence stereomicroscope at the designated times.

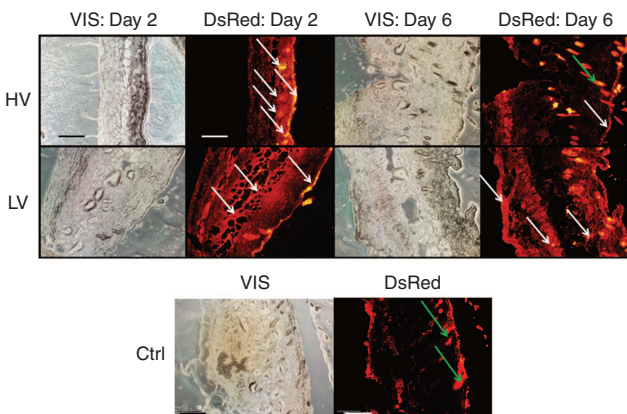


Figure 2 Depth of transfection of pCMV-DsRed into the skin after the application of high-voltage (HV) and low-voltage (LV) pulses. The fluorescence of DsRed in different skin layers was observed at day 2 and day 6 after the therapy in 20 μ m thick frozen skin sections using the fluorescence stereomicroscope. Areas with gene expression are marked with white arrows, and the green arrow represents the auto fluorescence of hair follicles. VIS, images were taken under visible light; Ctrl, control group with pCMV-DsRed injection, but without the electroporation. Scale bar: 200 μ m.

Pulse parameter choice is dependent on the transgene mode of action demonstrated in the wound-healing model

The wound-healing assay was used as a model for evaluating the effect of HV and LV pulses on the therapeutic

outcome of GET. The efficiency and the mechanisms of action of all the plasmids used in the experiment were evaluated and described elsewhere.^{12,13,22,25–27} For this study, they were selected based on already established mechanisms of action and were used as a model molecules. Three different plasmids with antiangiogenic action were selected, encoding IL-12, shRNA against melanoma cell adhesion molecule (MCAM) and shRNA against endoglin. As described above, IL-12 is responsible for local and systemic immunomodulation and the antiangiogenic effect of the therapy. The delivery of shRNA against endoglin, as well as the expression of shRNA against MCAM, typically has local, targeted vascular effects, as has been shown in previous studies of tumor models.^{25–27} The plasmid encoding the peptide LL-37 was used as a positive control because this peptide promotes the wound-healing process.¹² The model is based on the theory that antiangiogenic molecules interfere with the revascularization and reepithelialization of the skin and would slow down the healing process. A longer healing time after therapeutic plasmid delivery would indicate a higher gene expression and GET efficiency.

According to our results, the average time for complete wound repair is 14.2 ± 0.4 days, as observed after treatment with miliQ water or pControl delivery. Electroporation with LV pulses significantly prolonged wound-healing time in the group treated with IL-12 (Figure 5a). After the IL-12 delivery and the application of LV pulses, complete wound repair was achieved after 17.1 ± 0.9 days, *i.e.*, 3 days longer than in the

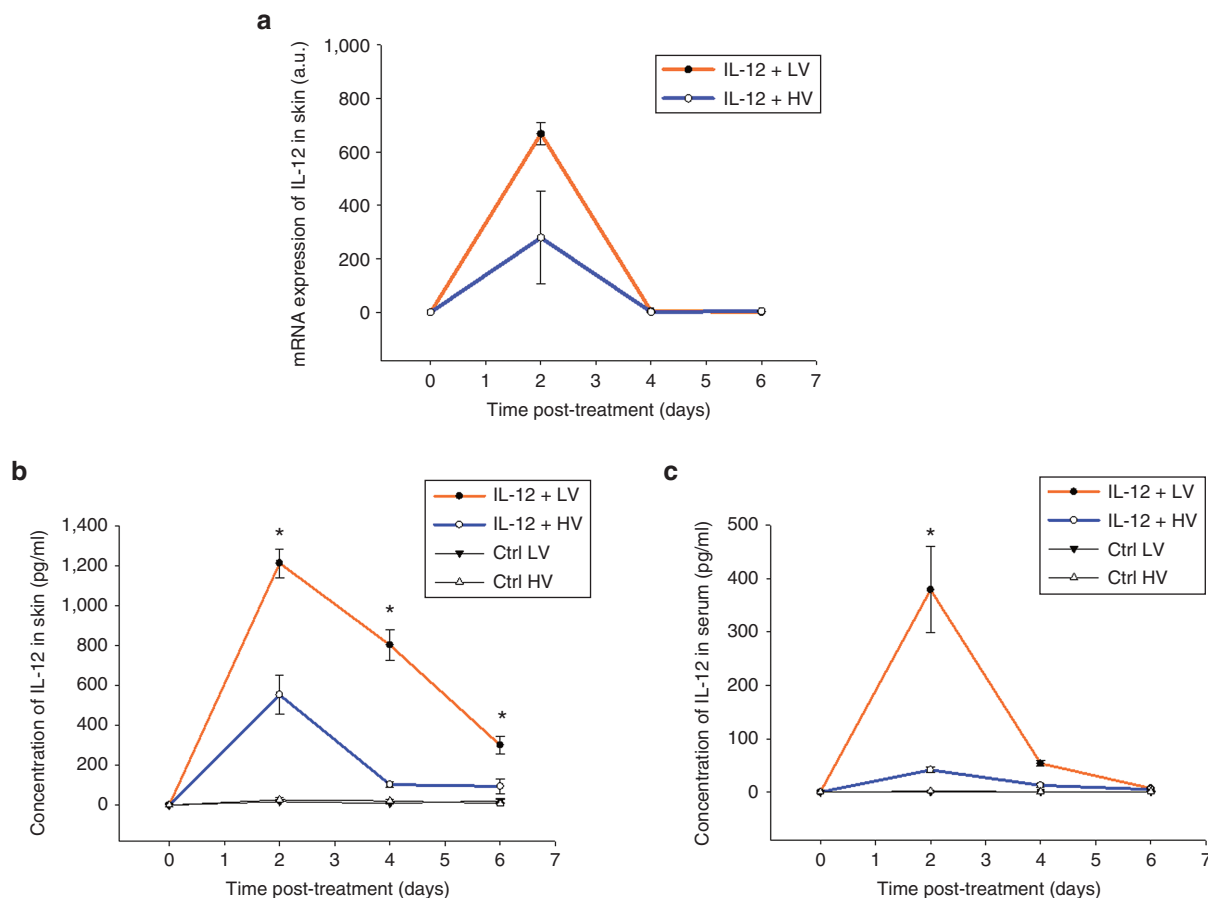


Figure 3 IL-12 mRNA and protein expression levels measured in skin and serum samples. (a) mRNA expression of IL-12 in skin samples. Real-time PCR analysis was performed at days 2, 4, and 6 post-treatment. (b) The concentration of IL-12 (pg/ml) measured in skin samples. The protein production was measured by ELISA at days 2, 4, and 6 after the treatment. (c) The concentration of IL-12 (pg/ml) measured in serum samples. The IL-12 protein was detected in the serum only after the administration of LV pulses and not after the application of HV pulses. The values are expressed as the arithmetic mean \pm standard error of the mean; **P* value indicates a significant difference ($P < 0.05$) between the groups treated either with LV or HV pulses. IL-12 + LV, intradermal injection of pORF-mIL-12 followed by the application of LV pulses; IL-12 + HV, intradermal injection of pORF-mIL-12 followed by the application of HV pulses; Ctrl LV or HV, intradermal injection of milliQ water followed by the application of LV or HV pulses.

control group (Figure 5b). Healing time after the treatment with IL-12 and the application of HV pulses did not differ from that of the control group. Electroporation with HV pulses prolonged wound-healing time in the group treated with shRNA against MCAM and in the group treated with shRNA against endoglin. Under the HV conditions, the healing time lasted 16.2 ± 0.9 days in the group treated with anti-endoglin shRNA and 19.0 ± 2.9 days in the group treated with anti MCAM shRNA. Wound healing was not significantly improved in those two groups after the delivery of LV pulses. Electroporation of pHCAP-18/LL-37 under the LV conditions led to earlier wound closure and a healing process that was up to 3 days shorter than that of the control groups (Figure 5b).

The results indicate that all the therapeutic approaches had antiangiogenic effectiveness; however, due to different modes of action, their therapeutic effectiveness was varied with different electrotransfer parameters. The effectiveness of IL-12 is mediated systemically and was greater with LV pulses that transfected deeper skin layers, whereas the effectiveness of shRNA against endoglin and MCAM is mediated locally and was greater with HV pulses. GET with pHCAP-18/LL-37 as a

positive control efficiently decreased healing time. In addition, better responses were observed under LV conditions, indicating that the optimal effectiveness of the peptide occurs when deeper skin layers are transfected, similarly as with IL-12.

Evaluation of skin damage

Electroporation side effects were evaluated by macroscopic observation of skin damage caused by the application of HV or LV pulses at days 2, 7, and 14 after the treatment. Examination of the treated skin areas revealed no skin damage after the application of HV pulses (Figure 6a). There was no topical skin damage at days 2 and 7 post-treatment. Fourteen days after the application of HV pulses, hair had completely regrown in the treated area. On the contrary, the application of LV electric pulses (Figure 6b) caused noticeable skin damage (hyperkeratosis) observed at day 2 post-treatment. The damage was observed in the hexagonal pattern, indicating that mild skin burns had occurred under each electrode pin (Figure 6c). The damage was not severe and had completely healed in 14 days. However, no hair regrew in the treated regions where the pins had contacted the skin.

Under the same electrical conditions, the experiment was repeated with the application of the conductive gel on the mouse skin before the pulses were applied; this was done both to avoid thermal skin damage and to improve the contact between the electrodes and the tissue.^{11,12,28,29} The use of conductive gel did not affect the degree of the skin damage, as observed in a series of treated animals (Figure 6b), indicating that the addition of conductive gel placed on the treated skin region did not ameliorate the skin damage caused by the applied electric pulses. Exposure of the skin to the LV pulses caused the same skin damage that resulted without the application of conductive gel. Once again, the HV pulses did not cause any noticeable skin damage.

The histological analysis of the treated skin (Figure 6d) revealed mild skin damage, which was mainly present in the epidermis. The treatment with HV pulses resulted in minor keratinocyte damage observed 2 days after the treatment. The thicker epithelium that was observed 6 days after pulse application indicates active recovery of the epidermis^{30,31} after the damage caused by the electric pulses. The keratinocyte damage was more evident after the application of LV pulses; as the LV pulses were more harmful to the skin cells, the thickness of the epithelium indicates extensive recovery of the epidermal cells. Histological analysis confirmed the macroscopically observed hair regrowth. The HV application led to normal hair regrowth, while the application of LV pulses destroyed the hair follicles underneath where the electrode pins were in contact with the skin.

Discussion

Our study shows that with different electrical pulses applied by noninvasive pin electrodes, the depth of transfection and the level of gene expression can be controlled. Therefore, we can optimize the electrotransfer parameters for different medical applications and adjust the pulses for local or systemic action of a transgene.

Electrotransfer parameters regulate the depth of transfection in the skin, duration of the gene expression, and local or systemic protein distribution

A large variety of pulses have been used for GET. The optimal pulse conditions reported are not the same for all applications, but they could depend on the type of tissue, type of electrode and injected DNA.⁵ The electric pulses chosen for gene transfection into skin have been either short duration (~100 μ s) HV pulses alone,^{2,32} long duration (>100ms) LV pulses alone,³³ or a combination of one or several HV and LV pulses.^{4,9,34,35} The amplitude and the duration of electric pulses used for GET are two critical parameters, which can affect the efficiency transgene expression as well as tissue damage.³⁶ Based on these published studies, we decided to test two different types of electric pulses, short HV pulses with an amplitude-over-distance ratio of 1600V/cm and duration 100 μ s, and long LV pulses with an amplitude-over-distance ratio of 170V/cm and duration 150ms. They were selected based on their efficiency to promote the local or systemic delivery of small molecules into the skin, as was demonstrated in our previous study.¹⁷

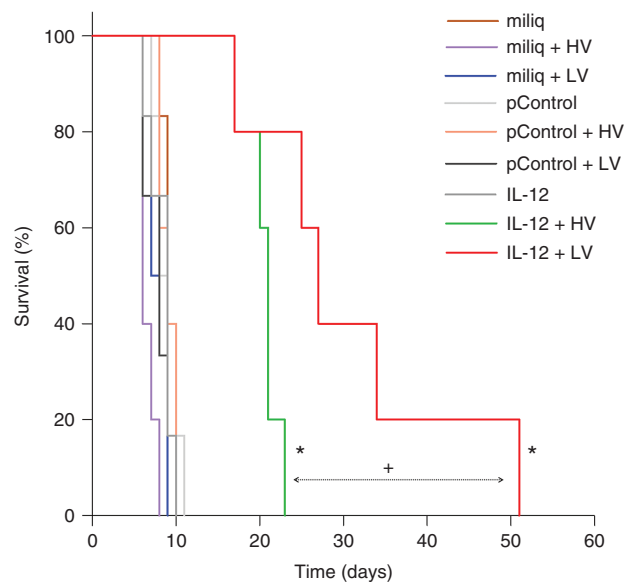


Figure 4 Mouse survival curves after treatment of the B16F10 melanoma tumors. **P* value indicates a significant increase ($P < 0.05$) in mouse survival observed either with IL-12 + HV or IL-12 + LV treatment compared with the untreated control group and the group treated with pControl. +*P* value indicates statistically a significant difference ($P < 0.05$) between the IL-12 + HV and IL-12 + LV groups. pControl, intradermal injection of control plasmid; IL-12, intradermal injection of pORF-mIL-12; LV, application of low-voltage pulses; HV, application of high-voltage pulses.

The results of this study showed the differences in the depth of transfection of plasmids into mouse skin resulting from using LV or HV electric pulses for GET. Specifically, the use of HV pulses promoted the transfection in upper skin layers (*i.e.*, epidermis and dermis), while the use of LV pulses promoted the transfection of deeper layers of the skin with muscle cells (*i.e.*, *panniculus carnosus*). The targeted transfection of different skin layers by the application of short HV or long LV pulses was demonstrated for the intradermal delivery of a reporter plasmid encoding DsRed, as well as for a therapeutic plasmid encoding IL-12. The transfection of cells in deeper layers of the skin achieved by LV pulses resulted in longer expression of the plasmid DNA with systemic distribution of the transcribed protein, as was demonstrated by the elevated serum levels of IL-12 at day 2 post-treatment. On the contrary, the transfection of cells in the epidermis and dermis that was achieved after the application of HV pulses resulted in local expression of the transgene without any systemic distribution. Therefore, electrotransfer parameters could regulate the depth of transfection in the skin and could essentially contribute to the duration of gene expression as well as regulate the local or systemic distribution of the transcribed protein (Figure 7). The therapeutic relevance of different electrotransfer parameters was presented with the B16F10 tumor treatment and the wound healing was performed as a proof of principle of variable effects of electrical conditions.

The mode of action of the delivered molecule requires the proper selection of HV or LV pulses

Different therapeutic plasmids have been transfected into skin via electrotransfer.^{5,14} Transgene molecules differ in mode of action as well in the dosage needed for optimal

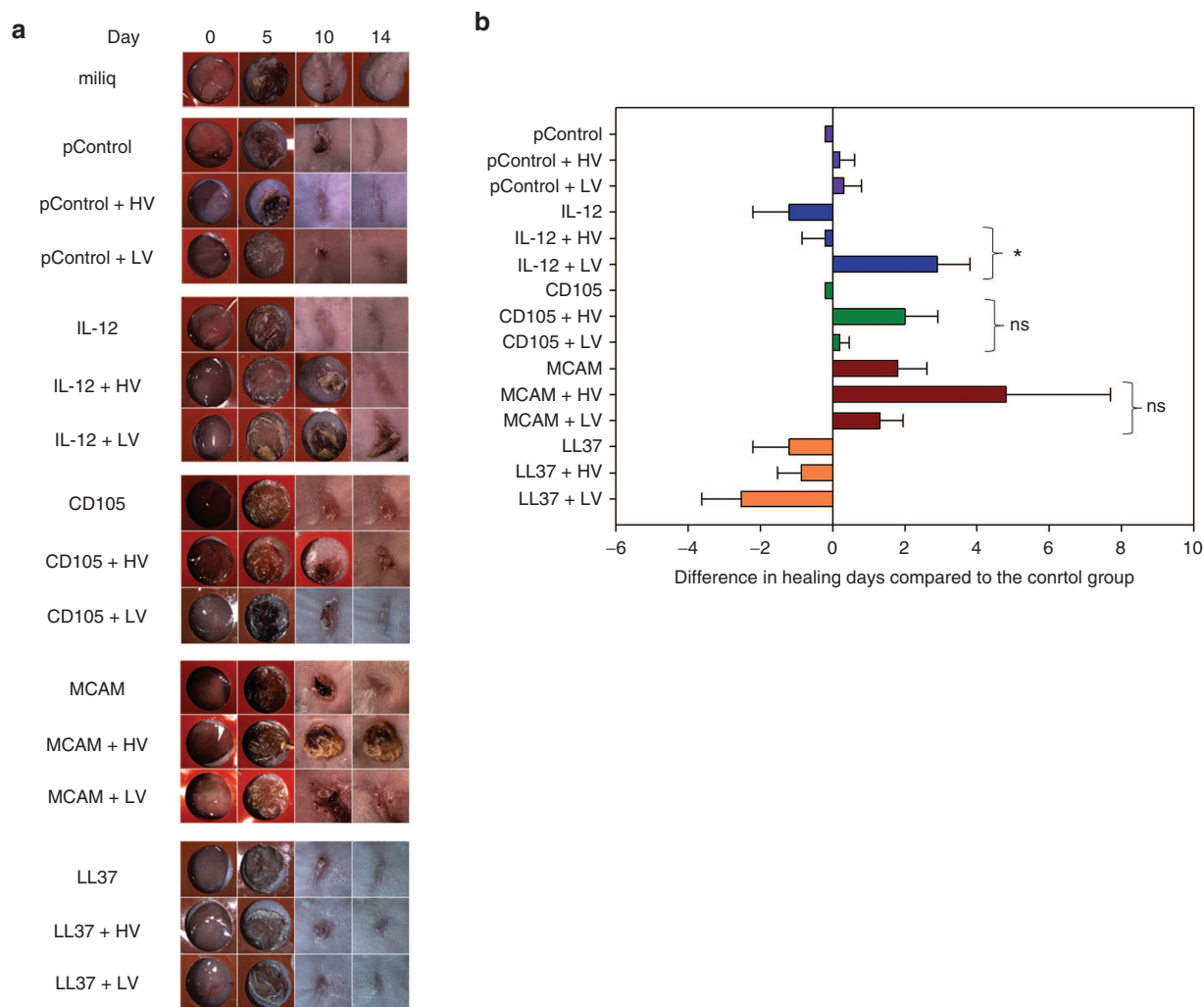


Figure 5 Therapeutic effect of plasmid DNA delivery after the application of HV or LV pulses. (a) Images of the wounds were captured with the digital camera connected to the stereomicroscope at the designated times. Wounds were created using a 5 mm round skin biopsy punch. The inner diameter of the red silicone ring is 6 mm. **(b)** To quantify the results of the wound-healing model, the wound images were analyzed using AxioVision software. The results are expressed as the number of days for complete wound repair, normalized to the control group. Error bars indicate standard error of the mean. **P* value < 0.05 between the selected groups; ns, no statistically significant difference between the groups; pControl, intradermal injection of control plasmid pControl; IL-12, intradermal injection of pORF-mIL-12; CD105, intradermal injection of pU6-antiCD105, coding for shRNA against endoglin (CD105); MCAM, intradermal injection of pU6-antiMCAM, coding for shRNA against melanoma cell adhesion molecule (MCAM); LV, application of low-voltage pulses; HV, application of high-voltage pulses.

therapeutic effectiveness. First, molecules delivered intradermally can act locally in the skin or elicit systemic effects when the products reach the bloodstream. As presented in this study, it is of the utmost importance to select the optimal electrical parameters according to the mode of action of the transcribed molecule. We demonstrated that for plasmids encoding molecules with a local mode of action, such as shRNA against endoglin^{26,27,37–39} or shRNA against MCAM,²⁵ the best effectiveness was obtained with HV pulses, which transfect the cells in the superficial mouse skin layers. In that way, the HV pulses would restrict the distribution of molecules with a local mode of action locally in the skin, thus avoiding possible systemic side effects due to their distribution in the bloodstream. In contrast, with molecules that have paracrine and systemic modes of action, such as IL-12, we obtained better effectiveness with LV pulses that promote the

transfection of deeper skin layers. Compared with HV pulses in the wound-healing model, better IL-12 effectiveness was obtained with LV pulses, which were required to achieve optimal systemic effects. Furthermore, the prolonged survival of B16F10 tumor-bearing mice clearly indicates an antitumor effectiveness of IL-12 with LV pulses applied in the peritumoral area than that resulting from the HV conditions.

Aside from the types of transfected cells, the optimal therapeutic effectiveness of gene therapy also depends on the amount of produced therapeutic transgene and the duration of expression. Therefore, the dosing needs to be optimized for each specific therapeutic plasmid. Although there have been several studies that have attempted to improve the dosage of plasmid DNA available for gene expression in the skin, the highest possible dosage does not always lead to the best therapeutic results.⁴⁰ Therefore, to reach optimal therapeutic

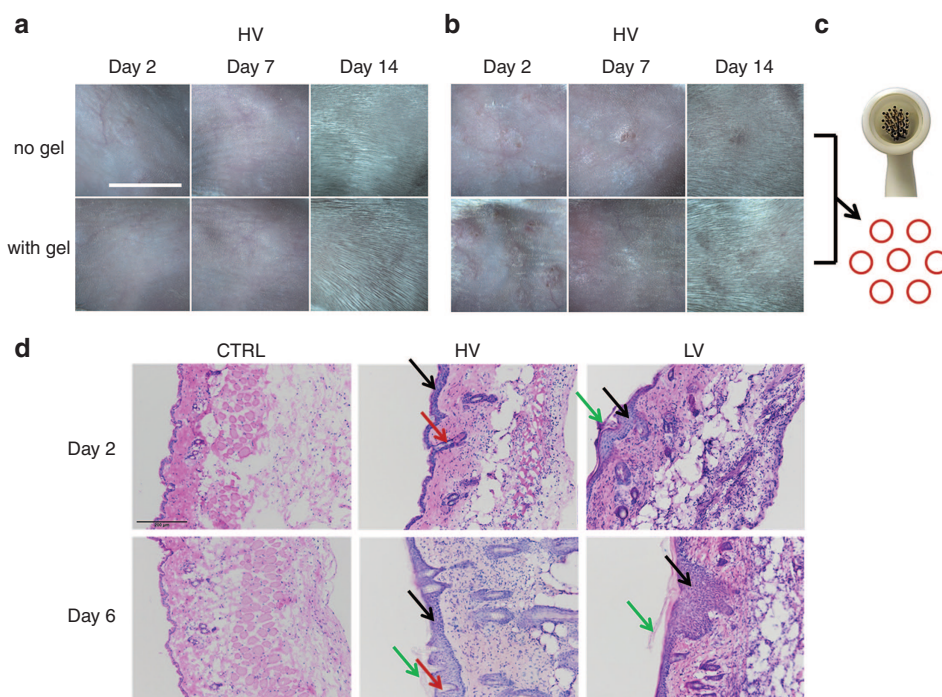


Figure 6 Macroscopic and microscopic evaluation of skin damage. Damage was observed after multiple milliQ injections followed by the application of (a) high-voltage (HV) pulses or (b) low-voltage (LV) pulses. Pulses were applied immediately after the intradermal injection of milliQ water (no gel) or after the preliminary administration of conductive gel (with gel). Mouse skin was observed under the stereomicroscope 2, 7, and 14 days after the application of HV and LV pulses. For each experimental condition, four treated skin areas were evaluated. Representative images of the skin damage in the treated region. Scale bar 5 mm. (c) Skin damage caused by LV pulses was observed in the same hexagonal pattern as that of the pins inside the MEA. Scale bar 5 mm. VIS images were taken under visible light. (d) Histological evaluation of skin damage. Skin sections were excised at day 2 or day 6 post-treatment and stained with hematoxylin and eosin. The keratinocyte damage is marked with green arrows, the extended thickness of epithelium is marked with black arrows, and the hair follicles are marked with the red arrows. Scale bar 200 μm . LV, low-voltage pulses; HV, high-voltage pulses; CTRL, untreated group.

effectiveness of GET, the level and duration of expression of the transgene transfected into the skin should be precisely regulated. The results of our study provide the evidence that with noninvasive electrodes and different electrotransfer parameters, the depth of skin transfection can be controlled, resulting in different levels and durations of IL-12 expression.

From mouse skin to clinical practice

Due to the specific structure of mouse skin with the subcutaneous *panniculus carnosus* muscle layer, mouse skin was selected as a model to assess the effect of different electrical parameters. The differential characteristics of mouse skin layers, including the muscle layer, provide an easy means of detecting the depth at which a transgene is expressed. Although only rudimentary forms of this subcutaneous muscle layer can be found in humans, such as in the small muscles of the face and neck or the platysma,¹⁵ the results of this study provide clear evidence that the parameters of electrotransfer influence the depth of transfection into the skin. Targeting deeper skin layers with LV pulses would lead to the transfection of cells with slower turnover, such as muscle cells, and thus, longer duration of gene expression. Because deeper, well-vascularized skin layers are transfected with LV pulses, the resulting systemic effect could be expected, even in the absence of the *panniculus carnosus* in human skin. The use of different electrical parameters, which regulate the depth of

transfection and distinguish between local or systemic response, would contribute to the translation of therapeutic GET into the clinic. These parameters present a promising tool for improving the safety and effectiveness of GET for various medical applications, such as wound healing, vaccination and cancer therapy. As demonstrated in this study, the electrical conditions should be carefully selected for each application. For instance, for the purposes of vaccination, which targets the local immune response of the skin cells, the HV pulses would optimally improve local gene expression in the skin. A similar example is the application of HV pulses in the wound-healing process, where a transgene should act locally, or in the paracrine mode. In that case, it is sufficient for the transgene to affect the local environment, as there is no need for a systemic response.¹⁴

On the other hand, LV pulses would be recommended for the delivery of molecules with systemic action and expected abscopal effects. One example is the delivery of plasmid DNA encoding IL-12 in cancer therapy,^{3,23,41–43} as was also demonstrated in our study. One specific promising approach is the administration of plasmid DNA encoding IL-12 peritumorally into skin to boost the immune reaction of the local ablative techniques.^{13,44} Such an approach was already proposed for electrochemotherapy in combination with IL-12 delivered by electrotransfer peritumorally and demonstrated effectiveness in client-owned dogs with spontaneous mast cell tumors.⁴⁴

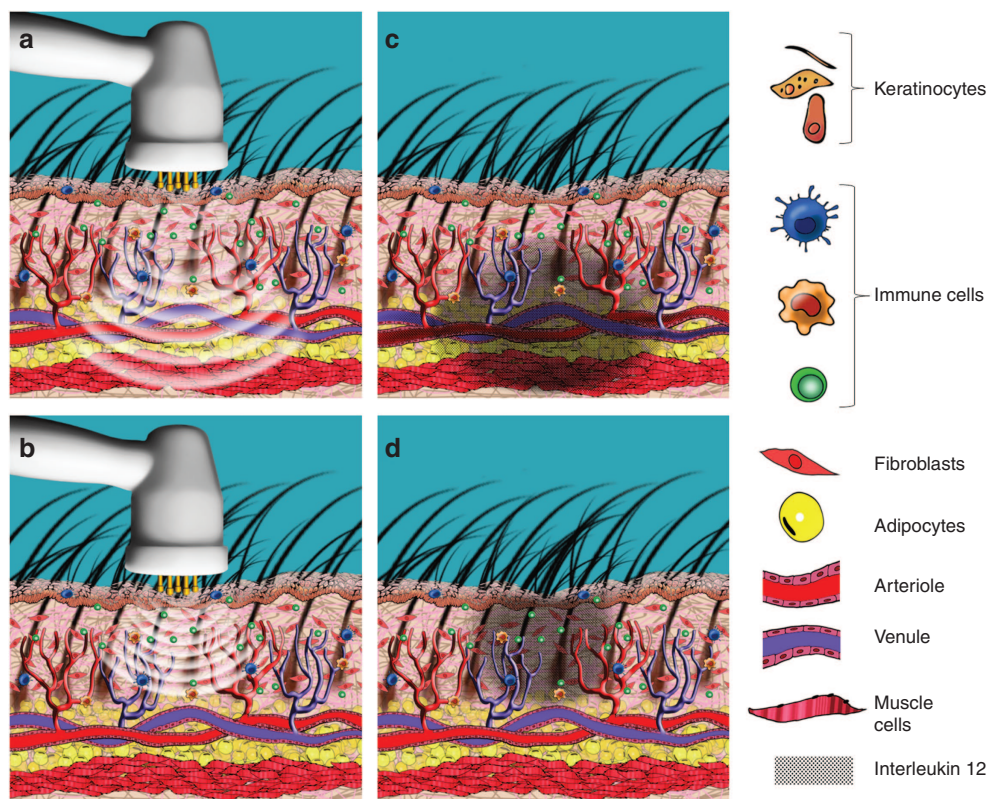


Figure 7 The depth of transfection in mouse skin and transgene distribution after high-voltage (HV) or low-voltage (LV) pulses, applied by MEA. LV pulses promote the transfection of deeper skin layers (a), while HV pulses promote the transfection of cells in the superficial layers of mouse skin (b). The deeper transfection achieved by LV pulses resulted in longer plasmid DNA expression with systemic protein distribution, as was demonstrated by the increased IL-12 serum levels (c). The transfection of the superficial skin layers by the HV pulses resulted in local plasmid DNA expression without any systemic transgene distribution (d).

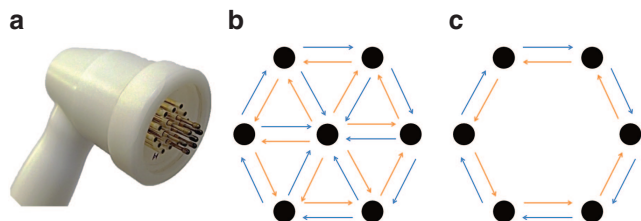


Figure 8 The distribution of electric pulses within the multi-electrode array (MEA). (a) Applicator of noninvasive MEA. (b) The electrode consists of seven spring-loaded pins arranged in a hexagonal mesh and spaced 3.5 mm apart. When the central pin was inserted, a total of 24 electric pulses (2 electric pulses between each electrode pair) were delivered during the treatment. (c) For wound healing and tumor treatment, the central pin was removed from the applicator; 6 pins remained on the electrode, delivering 12 electric pulses (2 electric pulses between each electrode pair).

MEA for the delivery of genes into the skin

Different types of electrodes have been used to deliver genes into the skin, from needle electrodes^{45,46} microneedles,⁴⁷ and plate electrodes^{36,48} to the more recent noninvasive MEA.^{49,50} One of the novelties of our study is the utilization of the circular MEA for wound healing and tumor treatment. In previous studies, the use of MEA was effective for the delivery of model drugs (e.g., dextran, fentanyl and doxorubicin),¹⁷ as well as plasmid DNA, into mouse skin³² with minimal skin damage caused by

electric pulses.¹⁷ Particularly the HV pulses provided harmless gene delivery, without noticeable skin damage. Although the LV pulses could result in more evident skin damage, potentially caused by longer pulse duration, the damage was not severe and had completely healed in 14 days. Therefore, the skin damage is not critical component to pulse selection and the use of the LV pulses should not cause the concerns for further application. The advantage of the MEA is that the number of addressable electrode pairs that are contained within the electrode applicator can be adjusted,⁵¹ which was also demonstrated in the current study with the removal of the central pin. As demonstrated by our results, the use of MEA with adjustable pins represents a valuable approach for the effective delivery of genes into the skin for wound healing, as well as for peritumoral delivery for cancer gene therapy. Hence, MEA opens the new possibilities to control the gene expression in the skin, which were not described for any other type of electrode so far.

Conclusion

Different skin layers and controlled gene expression in the skin can be achieved by selecting the appropriate electrotransfer parameters. Specifically, the application of LV or HV pulses provides the possibility to control depth and, consequently, the types of cells transfected; in this way, the systemic or local action of the transgene can also be controlled. Therefore, in the translation into the clinics, it will be of the

utmost importance to adjust the parameters of GET for different therapeutic approaches, desired therapeutic genes and their modes of action.

Materials and methods

Plasmids. The plasmids used for the experiments include the reporter plasmid encoding the *Discosoma* red fluorescent protein (DsRed), the control plasmid (pControl), and the therapeutic plasmids encoding hCAP-18/LL-37, interleukin 12 (IL-12), shRNA against MCAM, and shRNA against endoglin (CD105). The DsRed reporter gene was encoded on the pCMV-DsRed-Express2 plasmid (Clontech, Basingstoke, UK), and the mouse IL-12 gene was encoded on the pORF-mIL-12 plasmid (InvivoGen, Toulouse, FR). The precise construction of the control plasmid without the therapeutic gene (pControl)⁵² and the plasmids against MCAM (pU6-antiMCAM)²⁵ and against endoglin (pU6-antiCD105)²⁷ is described in our previous studies. The construction of the plasmid encoding hCAP-18/LL-37 is described elsewhere.¹² All plasmids were isolated using the EndoFree Plasmid Mega Kit (Qiagen, Hilden, DE) according to the manufacturer's instructions and diluted in endotoxin-free water (miliQ) to a concentration of 2 mg/ml. Plasmid DNA concentration and purity were determined both spectrophotometrically (Epoch Microplate Spectrophotometer; Take3 Micro-Volume Plate, BioTek, Bad Friedrichshall, DE) and by gel electrophoresis.

Animal ethics. All procedures were performed in compliance with the guidelines for animal experiments of the EU directive (2010/63/EU) and with permission from the Veterinary Administration of the Ministry of Agriculture, Forestry and Food of the Republic of Slovenia (permission no. 34401-4/2012/4, 34401-1/2015/7). Animals were housed in pathogen-free conditions with 12-hour light cycles and were provided food and water *ad libitum*.

In vivo GET and transfection efficiency. In the experiments, 8–12-week-old female BALB/c mice (Envigo, Udine, IT) weighing between 20 and 25 g were used; three to five mice were randomly assigned into each experimental group. One day prior to the experiments, the mice were shaved on the left and/or right flank, and any remaining hair was removed with depilatory cream (Veet Sensitive Skin, Reckitt Benckiser, UK). Before the plasmid injections, the mice were anesthetized in the induction chamber using 2% isoflurane (Nicholas Piramal India, London, UK) in oxygen, and they remained under isoflurane anesthesia during the procedure.

To observe the intensity and duration of gene expression in the skin, the anesthetized mice received multiple intradermal injections ($4 \times 20 \mu\text{l}$) of pCMV-DsRed (2 mg/ml) in the right and/or left flank. A 29-G insulin grade syringe (Terumo, Terumo Europe N.V., Leuven, BE) was used for the plasmid injection. To evaluate transfection depth, single intradermal and subcutaneous injections of $50 \mu\text{l}$ of pCMV-DsRed (2 mg/ml) were administered during the experiments, immediately after the plasmid injection electric pulses were applied. Two different electrotransfer parameters were used for plasmid delivery: either HV electric pulses with an amplitude-to-distance ratio of 1,600 V/cm (amplitude 570 V, duration of

pulse 100 μs) or LV electric pulses with an amplitude-to-distance ratio 170 V/cm (amplitude 60 V, duration 150 ms). GET was performed using a noninvasive MEA (Iskra Medical, Podnart, SI) consisting of seven spring-loaded pins arranged in a hexagonal mesh (Figure 8a,b) and spaced 3.5 mm apart. The MEA was gently pressed directly onto the depilated skin without the application of conductive gel. Due to the fact that the array was designed based on the commercially available hexagonal electrode from IGEA, the MEA was connected to the Cliniporator (IGEA s.r.l., Carpi, IT). A total of 24 electric pulses (2 electric pulses between each electrode pair in opposite direction) were delivered during the treatment. Expression of DsRed was monitored using a Zeiss SteREO Lumar.V12 (Zeiss, Jena, DE) fluorescence stereomicroscope equipped with an MRc5 digital camera (Zeiss). The mice were initially anesthetized with inhalation anesthesia in the induction chamber (2% of isoflurane in oxygen) and were then placed under the microscope with their snout in the inhalation tube to remain anesthetized during the measurement procedure. The mice were imaged daily from day 1 after the GET until the fluorescence was undetectable. A threshold suitable for the images was applied, and the fluorescence intensity in the area of the electroperated skin was determined using AxioVision software (Zeiss).

Histological determination of DsRed distribution and skin damage. For the histological determination of DsRed distribution in the skin, frozen sections were prepared. The mice received a single intradermal injection of $50 \mu\text{l}$ of pCMV-DsRed (2 mg/ml) in the left or right flank, and the electrotransfer was performed as described above. At day 2 and day 6 post-treatment, the mice were humanely sacrificed, and the region of the skin exposed to the treatment was excised. The excised skin was immediately frozen in liquid nitrogen. Subsequently, skin samples were embedded in medium designed for frozen tissue specimens (Tissue-Tek 4583, Sakura Finetek Europe B.V., Alphen aan den Rijn, NL), and $20 \mu\text{m}$ thick sections were cut in the direction perpendicular to skin layers. Additionally, some samples were fixed in zinc fixative (BD PharMingen, BD Bioscience, San Diego, CA) for 1 day and then stored in 70% ethanol until being embedded in paraffin for assessing skin damage histologically; $5 \mu\text{m}$ thick sections were cut in the direction perpendicular to the skin layers and stained with hematoxylin and eosin. The samples were observed using a BX-51 fluorescence microscope (Olympus, Hamburg, GE) equipped with a digital camera DP72 (Olympus).

Total mRNA extraction and quantitative reverse transcription polymerase chain reaction (qRT-PCR) analysis. The BALB/c mice received multiple intradermal injections ($4 \times 20 \mu\text{l}$) of pORF-mIL-12 in the left or right flank. Electric pulses were applied immediately after plasmid administration, as described above. The control group received intradermal injections of miliQ water, followed by electric pulses. To determine IL-12 expression in the mouse skin, RNA extraction and qRT-PCR analysis were performed at days 2, 4, and 6 after GET of pORF-mIL-12. The mice were sacrificed, and the treated skin regions were excised and snap-frozen in liquid nitrogen. Skin samples were later homogenized, and total

RNA was extracted with the TRIzol Plus RNA Purification system (Life Technologies, Carlsbad, CA), according to the manufacturer's instructions. RNA concentration and purity were determined spectrophotometrically (Epoch Microplate Spectrophotometer; Take3TM Micro-Volume Plate, BioTek, Bad Friedrichshall, DE). cDNA transcription was performed using 1,000 ng of total RNA extract using a SuperScript VILO cDNA Synthesis Kit (Life Technologies), according to the manufacturer's instructions. For the qRT-PCR analysis, mixtures of transcribed cDNA diluted 10-fold were used as templates using SYBR Select master Mix (Life Technologies). Custom primers (forward primer sequence: 5'-CGGCAG-CAGAATAAATATGAG-3', reverse primer sequence: 5'-GAG TTCTTCAAAGGCTTCATC-3') were designed to amplify the fragments of mouse IL-12 cDNA. The reaction was performed using a QuantStudio 3 analyzer (Applied Biosystems, Life Technologies), and the products were analyzed with the associated QuantStudio Design & Analysis Software (Life Technologies). The optimized thermal cycling conditions were as follows: activation of uracil-DNA glycosylase (2 minutes at 50 °C), hot start activation of AmpliTaq Gold Enzyme (10 minutes at 50 °C), 45 cycles of denaturation (15 seconds at 95 °C), annealing and extension (1 minute at 60 °C). The IL-12 mRNA expression levels in mouse skin are presented as the threshold cycle value (C_t). The relative quantification of cDNA expression was normalized to β -actin and glyceraldehyde 3-phosphate dehydrogenase (GAPDH) by the $2^{-\Delta\Delta C_t}$ method, calculated via the QuantStudio 3 software (Applied Biosystems, Life Technologies).

Quantification of IL-12 protein concentration. The concentration of the cytokine IL-12 was measured in excised skin and serum samples. BALB/c mice were treated as they were for the qRT-PCR analysis. At days 2, 4, and 6 post-treatment, the mice were sacrificed, and the treated region of the skin was excised, immediately weighed and snap-frozen in liquid nitrogen. The frozen samples were mechanically macerated. Each sample received 500 μ l of PBS containing protease inhibitors (Complete Protease Inhibitor Cocktail Tablets, Roche, Basel, CH); the samples were then thoroughly mixed and centrifuged for 10 minutes at 3,000 rpm. The supernatant was separated from the sediment and stored at -80 °C until further analysis. Blood was collected from the intraorbital sinus into a blood collection tube (Vacuette serum tube with gel; Greiner Bio-One International AG, Kremsmünster, AU) and stored at 4 °C for 20 minutes until it had coagulated. Serum was extracted from the blood samples via centrifugation at 2,500 rpm for 5 minutes, and the serum was immediately stored at -80 °C until further analysis. Both sets of samples were analyzed using enzyme-linked immunosorbent assay (ELISA) (ELISA Quantikine Mouse IL-12 p70 Immunoassay, R&D Systems, Minneapolis, MN). Due to the highly comparable mass of the samples, the IL-12 concentrations are presented as pg of IL-12 per ml of serum or ml of supernatant.

Evaluation of antitumor effectiveness. Tumors were induced by a subcutaneous injection of $1 \times 10^6/0.1$ ml of B16F10 melanoma cells into the right mouse flank; these cells are syngeneic to C57Bl/C mice (Envigo). The mice in this experiment were 8–10 weeks old, weighing between 18 and 20 g. When

the tumors reached an approximate volume of 40 mm³, the mice were randomly divided into experimental groups, and the treatments were administered; this point constituted day 0 of our study. The tumors were treated with multiple intradermal peritumoral injections (4×20 μ l) of pORF-mIL-12 in the concentration of 2 mg/ml; mice in the control group received milliQ water. Immediately after the plasmid injections, the peritumoral region was covered with conductive gel, and the LV or HV pulses were applied via an MEA with the central pin removed (Figure 8c). Thereafter, the tumors were measured in three perpendicular directions (a, b, c) every 2–3 days using a digital Vernier caliper. Tumor volume was calculated using the following formula: $V = a \times b \times c \times \pi/6$. The results are expressed using Kaplan-Meier curves; overall survival is presented as a percentage of mice present in the experiment at different time points post-treatment. The mice were sacrificed and disregarded from the experiment when the tumor reached a volume of 350 mm³.

Wound model and electroporation of wounded skin. BALB/c female mice (Envigo) weighing between 18 and 20 g were used in this experiment. At the time of treatment, the mice were 6–8 weeks old. Using the younger mice, it ensured that the skin structure was intact. The mice were anesthetized using an intraperitoneal injection of ketamine (1 mg/ml, Narektan, Vetoquinol, Ittigen, CH), xylazine (5 mg/ml, Chanazine; Chanelle Pharmaceuticals, Loughrea, IRL) and acepromazine (0.4 mg/ml, Promace; Fort Dodge Animal Health, Fort Dodge, IA). The injection volume was adjusted to the weight of the mouse and ranged from 70–90 μ l.

The dorsal surface was shaved and treated with depilatory cream (Veet Sensitive Skin) to remove any remaining hair. The dorsum of each anesthetized animal was disinfected with polyvidone iodine (Braunoderm, Braun, Melsungen, GE). Two full-thickness wounds, one on the each mouse flank, were created using a 5 mm, round skin biopsy punch (Kai Europe GmbH, Solinger, GE). To avoid cross-contamination, both wounds received the same treatment. Plasmids in a total volume of 80 μ l (160 μ g per mouse) were intradermally injected in four sites around each wound (4×20 μ l). Mice in the control group received injections of milliQ water. Each wound was caught in between MEA, consisting of six spring-loaded pins (Figure 8c) spaced 3.5 mm apart, and the Cliniporator (IGEA s.r.l., Carpi, IT) was used. The same electrodes were used as described in the previous experiment, this time with the central pin removed.⁵¹ Both HV and LV pulses were tested. To reduce wound contraction, the wounds were fixed with silicone splints that had been cut from a 0.5 mm thick silicone sheet (Grace Bio-Labs, Sigma-Aldrich). Donut-shaped splints with an outer diameter of 15 mm and an inner diameter of 6 mm were placed around each wound so that the wound was centered within the splint. An immediate-bonding adhesive was applied to fix the splint to the skin, followed by 5-0 Mersilk, nonabsorbable sutures (Ethicon, San Lorenzo, Puerto Rico). The wounds were washed with saline and covered by nonadhesive patches (Tosama, Domzale, SI) and transparent, occlusive wound dressings (Tegaderm, Neuss, GE). After the surgery, the mice received intramuscular analgesia (butorphanol, 50 μ l of 3 mg/kg, Torbugesic; Fort Dodge Animal Health), which was repeated the next day. At days 0,

3, 5, 7, 10, and 14, the wounds were digitally imaged using a Zeiss SteREO Lumar.V12 (Zeiss, Jena, GE) fluorescence stereomicroscope equipped with an MRc5 digital camera (Zeiss). The same optical zoom was maintained throughout the experiment. If the treatment prolonged the healing process, the wounds were observed on additional days until the healing was completed. Wound area was quantified using the AxioVision software (Zeiss). The results are expressed as the percentage of wound coverage compared with day 0 postsurgery and are normalized to the control group treated with miliQ water or pControl.

Evaluation of skin damage caused by electric pulses. BALB/c mice received multiple intradermal injections ($4 \times 20 \mu\text{l}$) of miliQ water in the left or right flank. Immediately after the administration of miliQ water, HV or LV electric pulses were applied, as described in the section above. The application was performed with or without the conductive gel (AquaUltra Basic, Ultragel, Budapest, HU). Potential skin damage was assessed using the stereo microscope (Zeiss). The treated skin regions were digitally imaged at days 2, 7, and 14 post-treatment. Subsequently, the effect of different electrotransfer parameters on skin damage was compared; in addition, the effect of conductive gel for the prevention of potential skin damage was evaluated.

Statistical analysis. Sigma Plot software (Systat software, London, UK) was used for statistical analysis. Significance was determined by Student's *t*-test or one-way analysis of variance followed by the Holm-Sidak test. The analysis of survival after the tumor treatment was performed using the log-rank test. A $P < 0.05$ was considered significant. Values are expressed as the arithmetic mean \pm standard error of the mean.

Acknowledgments The authors acknowledge the financial support from the state budget for the Slovenian Research Agency (program no. P3-0003, projects no. J3-4211, J3-6793, J3-4259, J3-6796). The research was conducted in the scope of LEA EBAM (French-Slovenian European Associated Laboratory: Pulsed Electric Fields Applications in Biology and Medicine) and is a result of networking efforts within COST TD1104 Action. Gaëlle Vandermeulen is a postdoctoral researcher of the Fonds de la Recherche Scientifique-FNRS, Belgium. We would like to thank Iskra Medical d.o.o. for providing the multi-electrode array that was used in the experiments. We would like to thank Mira Lavric and Masa Bosnjak (Institute of Oncology Ljubljana, Ljubljana, Slovenia) for all the valuable work they contributed to this research.

1. Yarmush, ML, Golberg, A, Serša, G, Kotnik, T and Miklavčič, D (2014). Electroporation-based technologies for medicine: principles, applications, and challenges. *Annu Rev Biomed Eng* **16**: 295–320.
2. Drabick, JJ, Glasspool-Malone, J, King, A and Malone, RW (2001). Cutaneous transfection and immune responses to intradermal nucleic acid vaccination are significantly enhanced by *in vivo* electroporation. *Mol Ther* **3**: 249–255.
3. Heller, R, Schultz, J, Lucas, ML, Jaroszeski, MJ, Heller, LC, Gilbert, RA et al. (2001). Intradermal delivery of interleukin-12 plasmid DNA by *in vivo* electroporation. *DNA Cell Biol* **20**: 21–26.
4. Pavselj, N and Prät, V (2005). DNA electrotransfer into the skin using a combination of one high- and one low-voltage pulse. *J Control Release* **106**: 407–415.
5. Lambricht, L, Lopes, A, Kos, S, Sersa, G, Prät, V and Vandermeulen, G (2016). Clinical potential of electroporation for gene therapy and DNA vaccine delivery. *Expert Opin Drug Deliv* **13**: 295–310.
6. Dobaño, C, Wiedera, G, Rabussay, D and Doolan, DL (2007). Enhancement of antibody and cellular immune responses to malaria DNA vaccines by *in vivo* electroporation. *Vaccine* **25**: 6635–6645.
7. Medi, BM, Hoselton, S, Marepalli, RB and Singh, J (2005). Skin targeted DNA vaccine delivery using electroporation in rabbits. I: efficacy. *Int J Pharm* **294**: 53–63.
8. Roos, AK, Eriksson, F, Timmons, JA, Gerhardt, J, Nyman, U, Gudmundsdóttir, L et al. (2009). Skin electroporation: effects on transgene expression, DNA persistence and local tissue environment. *PLoS One* **4**: e7226.
9. Roos, AK, Eriksson, F, Walters, DC, Pisa, P and King, AD (2009). Optimization of skin electroporation in mice to increase tolerability of DNA vaccine delivery to patients. *Mol Ther* **17**: 1637–1642.
10. Ferraro, B, Cruz, YL, Coppola, D and Heller, R (2009). Intradermal delivery of plasmid VEGF(165) by electroporation promotes wound healing. *Mol Ther* **17**: 651–657.
11. Chereddy, KK, Her, CH, Comune, M, Moia, C, Lopes, A, Porporato, PE et al. (2014). PLGA nanoparticles loaded with host defense peptide LL37 promote wound healing. *J Control Release* **194**: 138–147.
12. Steinstraesser, L, Lam, MC, Jacobsen, F, Porporato, PE, Chereddy, KK, Becerikli, M et al. (2014). Skin electroporation of a plasmid encoding hCAP-18/LL-37 host defense peptide promotes wound healing. *Mol Ther* **22**: 734–742.
13. Sersa, G, Teissie, J, Cemazar, M, Signori, E, Kamensek, U, Marshall, G et al. (2015). Electrochemotherapy of tumors as *in situ* vaccination boosted by immunogene electrotransfer. *Cancer Immunol Immunother* **64**: 1315–1327.
14. Gonthelf, A and Gehl, J (2010). Gene electrotransfer to skin: review of existing literature and clinical perspectives. *Curr Gene Ther* **10**: 287–299.
15. Gerber, PA, Buhren, BA, Schrupf, H, Horney, E, Zlotnik, A and Hevezi, P (2014). The top skin-associated genes: a comparative analysis of human and mouse skin transcriptomes. *Biol Chem* **395**: 577–591.
16. Vandermeulen, G, Staes, E, Vanderhaeghen, ML, Bureau, MF, Scherman, D and Prät, V (2007). Optimisation of intradermal DNA electrotransfer for immunisation. *J Control Release* **124**: 81–87.
17. Blagus, T, Markelc, B, Cemazar, M, Kosjek, T, Preat, V, Miklavcic, D et al. (2013). *In vivo* real-time monitoring system of electroporation mediated control of transdermal and topical drug delivery. *J Control Release* **172**: 862–871.
18. Gonthelf, A and Gehl, J (2012). What you always needed to know about electroporation based DNA vaccines. *Hum Vaccin Immunother* **8**: 1694–1702.
19. Dean, DA (2013). Cell-specific targeting strategies for electroporation-mediated gene delivery in cells and animals. *J Membr Biol* **246**: 737–744.
20. Gonthelf, A, Hojman, P and Gehl, J (2010). Therapeutic levels of erythropoietin (EPO) achieved after gene electrotransfer to skin in mice. *Gene Ther* **17**: 1077–1084.
21. Guo, S, Israel, AL, Basu, G, Donate, A and Heller, R (2013). Topical gene electrotransfer to the epidermis of hairless guinea pig by non-invasive multielectrode array. *PLoS One* **8**: e73423.
22. Pavlin, D, Cemazar, M, Kamensek, U, Tozon, N, Pogacnik, A and Sersa, G (2009). Local and systemic antitumor effect of intratumoral and peritumoral IL-12 electrogene therapy on murine sarcoma. *Cancer Biol Ther* **8**: 2114–2122.
23. Sedlar, A, Dolinsek, T, Markelc, B, Prosen, L, Kranjc, S, Bosnjak, M et al. (2012). Potentiation of electrochemotherapy by intramuscular IL-12 gene electrotransfer in murine sarcoma and carcinoma with different immunogenicity. *Radiol Oncol* **46**: 302–311.
24. Tevz, G, Kranjc, S, Cemazar, M, Kamensek, U, Coer, A, Krzan, M et al. (2009). Controlled systemic release of interleukin-12 after gene electrotransfer to muscle for cancer gene therapy alone or in combination with ionizing radiation in murine sarcomas. *J Gene Med* **11**: 1125–1137.
25. Prosen, L, Markelc, B, Dolinsek, T, Music, B, Cemazar, M and Sersa, G (2014). Mcam silencing with RNA interference using magnetofection has antitumor effect in murine melanoma. *Mol Ther Nucleic Acids* **3**: e205.
26. Dolinsek, T, Markelc, B, Sersa, G, Coer, A, Stimac, M, Lavrenca, J et al. (2013). Multiple delivery of siRNA against endoglin into murine mammary adenocarcinoma prevents angiogenesis and delays tumor growth. *PLoS One* **8**: e58723.
27. Dolinsek, T, Markelc, B, Bosnjak, M, Blagus, T, Prosen, L, Kranjc, S et al. (2015). Endoglin silencing has significant antitumor effect on murine mammary adenocarcinoma mediated by vascular targeted effect. *Curr Gene Ther* **15**: 228–244.
28. Gehl, J, Sorensen, TH, Nielsen, K, Raskmark, P, Nielsen, SL, Skovsgaard, T et al. (1999). *In vivo* electroporation of skeletal muscle: threshold, efficacy and relation to electric field distribution. *Biochim Biophys Acta* **1428**: 233–240.
29. Miklavcic, D, Beravs, K, Semrov, D, Cemazar, M, Demsar, F and Sersa, G (1998). The importance of electric field distribution for effective *in vivo* electroporation of tissues. *Biophys J* **74**: 2152–2158.
30. Markelc, B, Bellard, E, Sersa, G, Pelofy, S, Teissie, J, Coer, A et al. (2012). *In vivo* molecular imaging and histological analysis of changes induced by electric pulses used for plasmid DNA electrotransfer to the skin: a study in a dorsal window chamber in mice. *J Membr Biol* **245**: 545–554.
31. Golberg, A, Khan, S, Belov, V, Quinn, KP, Albadawi, H, Felix Broelsch, G et al. (2015). Skin rejuvenation with non-invasive pulsed electric fields. *Sci Rep* **5**: 10187.
32. Kos, S, Tesic, N, Kamensek, U, Blagus, T, Cemazar, M, Kranjc, S et al. (2015). Improved specificity of gene electrotransfer to skin using pDNA under the control of collagen tissue-specific promoter. *J Membr Biol* **248**: 919–928.

33. Donate, A, Coppola, D, Cruz, Y and Heller, R (2011). Evaluation of a novel non-penetrating electrode for use in DNA vaccination. *PLoS One* **6**: e19181.
34. Vandermeulen, G, Richiardi, H, Escriou, V, Ni, J, Fournier, P, Schirmacher, V et al. (2009). Skin-specific promoters for genetic immunisation by DNA electroporation. *Vaccine* **27**: 4272–4277.
35. André, FM, Gehl, J, Sersa, G, Préat, V, Hojman, P, Eriksen, J et al. (2008). Efficiency of high- and low-voltage pulse combinations for gene electrotransfer in muscle, liver, tumor, and skin. *Hum Gene Ther* **19**: 1261–1271.
36. Heller, LC, Jaroszeski, MJ, Coppola, D, McCray, AN, Hickey, J and Heller, R (2007). Optimization of cutaneous electrically mediated plasmid DNA delivery using novel electrode. *Gene Ther* **14**: 275–280.
37. Dolinsek, T, Sersa, G, Prosen, L, Bosnjak, M, Stimac, M, Razborssek, U et al. (2016). Electrotransfer of plasmid DNA encoding an anti-mouse endoglin (CD105) shRNA to B16 melanoma tumors with low and high metastatic potential results in pronounced anti-tumor effects. *Cancers (Basel)* **8**(1), 3; doi: 10.3390/cancers8010003 **8**.
38. Stimac, M, Dolinsek, T, Lamprecht, U, Cemazar, M and Sersa, G (2015). Gene electrotransfer of plasmid with tissue specific promoter encoding shRNA against endoglin exerts antitumor efficacy against murine TSA tumors by vascular targeted effects. *PLoS One* **10**: e0124913.
39. Tesic, N, Kamensek, U, Sersa, G, Kranjc, S, Stimac, M, Lamprecht, U et al. (2015). Endoglin (CD105) silencing mediated by shRNA under the control of endothelin-1 promoter for targeted gene therapy of melanoma. *Mol Ther Nucleic Acids* **4**: e239.
40. Shirley, SA, Lundberg, CG, Li, F, Burcus, N and Heller, R (2015). Controlled gene delivery can enhance therapeutic outcome for cancer immune therapy for melanoma. *Curr Gene Ther* **15**: 32–43.
41. Cemazar, M, Jarm, T and Sersa, G (2010). Cancer electrogene therapy with interleukin-12. *Curr Gene Ther* **10**: 300–311.
42. Daud, AI, DeConti, RC, Andrews, S, Urbas, P, Riker, AI, Sondak, VK et al. (2008). Phase I trial of interleukin-12 plasmid electroporation in patients with metastatic melanoma. *J Clin Oncol* **26**: 5896–5903.
43. Lucas, ML, Heller, L, Coppola, D and Heller, R (2002). IL-12 plasmid delivery by *in vivo* electroporation for the successful treatment of established subcutaneous B16.F10 melanoma. *Mol Ther* **5**: 668–675.
44. Cemazar, M, Ambrozic Avgustin, J, Pavlin, D, Sersa, G, Poli, A, Krhac Levacic, A et al. (2016). Efficacy and safety of electrochemotherapy combined with peritumoral IL-12 gene electrotransfer of canine mast cell tumours. *Vet Comp Oncol* **10**.1111/vco.12208.
45. Gothelf, A, Mahmood, F, Dagnaes-Hansen, F and Gehl, J (2011). Efficacy of transgene expression in porcine skin as a function of electrode choice. *Bioelectrochemistry* **82**: 95–102.
46. Maruyama, H, Ataka, K, Higuchi, N, Sakamoto, F, Gejyo, F and Miyazaki, J (2001). Skin-targeted gene transfer using *in vivo* electroporation. *Gene Ther* **8**: 1808–1812.
47. Daugimont, L, Baron, N, Vandermeulen, G, Pavselj, N, Miklavcic, D, Jullien, MC et al. (2010). Hollow microneedle arrays for intradermal drug delivery and DNA electroporation. *J Membr Biol* **236**: 117–125.
48. Vandermeulen, G, Vanvarenberg, K, De Beuckelaer, A, De Koker, S, Lambricht, L, Uyttenhove, C et al. (2015). The site of administration influences both the type and the magnitude of the immune response induced by DNA vaccine electroporation. *Vaccine* **33**: 3179–3185.
49. Heller, R, Cruz, Y, Heller, LC, Gilbert, RA and Jaroszeski, MJ (2010). Electrically mediated delivery of plasmid DNA to the skin, using a multielectrode array. *Hum Gene Ther* **21**: 357–362.
50. Guo, S, Donate, A, Basu, G, Lundberg, C, Heller, L and Heller, R (2011). Electro-gene transfer to skin using a noninvasive multielectrode array. *J Control Release* **151**: 256–262.
51. Kos, S, Blagus, T, Cemazar, M, Jelenc, J, and Sersa, G (2015). Utilization of multi-array electrodes for delivery of drugs and genes in the mouse skin. *IFMBE Proceedings* **53**: 321–324.
52. Bosnjak, M, Dolinsek, T, Cemazar, M, Kranjc, S, Blagus, T, Markelc, B et al. (2015). Gene electrotransfer of plasmid AMEP, an integrin-targeted therapy, has antitumor and antiangiogenic action in murine B16 melanoma. *Gene Ther* **22**: 578–590.



This work is licensed under a Creative Commons Attribution-NonCommercial-NoDerivs 4.0 International License. The images or other third party material in this article are included in the article's Creative Commons license, unless indicated otherwise in the credit line; if the material is not included under the Creative Commons license, users will need to obtain permission from the license holder to reproduce the material. To view a copy of this license, visit <http://creativecommons.org/licenses/by-nc-nd/4.0/>

© The Author(s) (2016)